



D-Amino acid oxidase bio-functionalized platforms: Toward an enhanced enzymatic bio-activity



Elisa Herrera^a, Javier Valdez Taubas^b, Carla E. Giacomelli^{a,*}

^a Instituto de Físicoquímica de Córdoba (INFIQC-CONICET), Departamento de Físicoquímica, Facultad de Ciencias Químicas, Universidad Nacional de Córdoba, Ciudad Universitaria, 5000 Córdoba, Argentina

^b CIQUIBIC, Departamento de Química Biológica, Facultad de Ciencias Químicas, Universidad Nacional de Córdoba, 5000 Córdoba, Argentina

ARTICLE INFO

Article history:

Received 27 May 2015

Received in revised form 10 August 2015

Accepted 14 August 2015

Available online 18 August 2015

Keywords:

His-tag enzyme

Surface bio-activity

Adsorption mechanism

Electrochemical detection

ABSTRACT

The purpose of this work is to study the adsorption process and surface bio-activity of His-tagged D-amino acid oxidase (DAAO) from *Rhodotorula gracilis* (His₆-RgDAAO) as the first step for the development of an electrochemical bio-functionalized platform. With such a purpose this work comprises: (a) the His₆-RgDAAO bio-activity in solution determined by amperometry, (b) the adsorption mechanism of His₆-RgDAAO on bare gold and carboxylated modified substrates in the absence (substrate/COO⁻) and presence of Ni(II) (substrate/COO⁻ + Ni(II)) determined by reflectometry, and (c) the bio-activity of the His₆-RgDAAO bio-functionalized platforms determined by amperometry. Comparing the adsorption behavior and bio-activity of His₆-RgDAAO on these different solid substrates allows understanding the contribution of the diverse interactions responsible for the platform performance. His₆-RgDAAO enzymatic performance in solution is highly improved when compared to the previously used pig kidney (*pk*) DAAO. His₆-RgDAAO exhibits an amperometrically detectable bio-activity at concentrations as low as those expected on a bio-functional platform; hence, it is a viable bio-recognition element of D-amino acids to be coupled to electrochemical platforms. Moreover, His₆-RgDAAO bio-functionalized platforms exhibit a higher surface activity than *pk*DAAO physically adsorbed on gold. The platform built on Ni(II) modified substrates present enhanced bio-activity because the surface complexes histidine-Ni(II) provide with site-oriented, native-like enzymes. The adsorption mechanism responsible of the excellent performance of the bio-functionalized platform takes place in two steps involving electrostatic and bio-affinity interactions whose prevalence depends on the degree of surface coverage.

© 2015 Elsevier B.V. All rights reserved.

1. Introduction

Enzyme bio-functionalized platforms are of major importance in biosensing, drug delivery, and decontamination systems as well as in various industrial processes from pharmaceutical and food processing to waste treatment [1–3]. The challenge behind these applications is to integrate the highly specific molecular recognition of native enzymes to the platform. Enzymes adsorb to the majority of solid substrates, mainly through electrostatic and hydrophobic interactions [4–8]. Usually, hydrophobic interactions confer some degree of denaturalization to the adsorbed enzymes; thus attempts have been proposed to induce favorable electrostatic interactions. Since most of the used solids are

negatively charged at pH conditions in which enzymes are active, as well as many of the residues of the proteins (pH > IEP), different strategies have been recently proposed to confer positive charge to the solid substrates: pre-adsorption of metal ions [9], cationic polymers [10] or cationized proteins [11,12]. On the other hand, covalent bonds between the enzyme and the substrate also represent a way to minimize the protein denaturalization produced by physical (mostly hydrophobic and electrostatic) interactions [12]. However, covalent linkage requires the modification of one or both parties which may also affect the biological activity. In many cases, these methods give rise to high enzyme loadings maintaining the native structure and biological activity, even increasing the response of the adsorbed enzymes compared to the activity in solution [13–15]. However, none of these methods can control the orientation of the enzyme on the solid substrates, the other key factor that determines the enzyme performance in terms of active site accessibility. In this regard, the interaction between His-tag (usually His₆) proteins and surface metal

* Corresponding author. Tel.: +54 351 535 3866; fax: +54 351 433 4188.

E-mail addresses: giacomel@fcq.unc.edu.ar, carlaeg@gmail.com (C.E. Giacomelli).

sites (Ni^{2+} , Cu^{2+} , Co^{2+} , or Zn^{2+}) generates high-affinity surface chelate complex of oriented enzymes [16,17]. His-tags can be genetically introduced into recombinant enzymes at the N- or C-terminal as well as in exposed loops of the protein without affecting the biological activity [4,18]. Therefore, this bio-affinity reaction between the histidine residues of the protein and the cation on the surface offers a gentle site oriented bio-functionalization procedure, providing important advantages over other strategies [16,17,19,20].

Bio-affinity interactions between a His-tag antigen and Ni(II)-modified solid substrates (silica and gold) were proven to provide a very good performance of the bio-functional platform [21,22]. Bio-affinity interactions result in site-oriented antigens on the surface with a strong coordinate bond between the His-tag at the N-terminal of the protein and the Ni(II) surface sites which can only be removed with high concentration of specific competitors (i.e. histidine or imidazole solutions). The assembly is the result of two-stage competitive mechanism ruled by electrostatic interactions followed by the surface complex formation between the His-tag and Ni(II) sites. This two-stages process is controlled by the characteristic filling (τ_f) and optimization (τ_{op}) times, related to the first electrostatic approach and the bio-affinity interactions, respectively. The two time constants appear because of the small size of the tag compared to the whole antigen that limits the complex formation.

D-Amino acid oxidase (DAAO, EC 1.4.3.3) catalyses the oxidation of D-amino acids to the corresponding α -keto acids in the presence of O_2 to produce H_2O_2 and ammonia [23–28]. This redox reaction coupled to a DAAO bio-functionalized platform has been employed to detect D-amino acids with electrochemical biosensors [27,28], to treat tumors with the H_2O_2 produced *in vivo* from exogenous molecules [25] and to manufacture the mother nucleus of cephalosporin antibiotics [23]. Therefore, several solid substrates together with DAAO from different sources have been proposed to improve the enzymatic response of the bio-functionalized platforms. Recently, we studied the surface bio-activity of DAAO from pig kidney (*pkDAAO*) on negatively charged hydrophilic (silica) and hydrophobic (gold) solid substrates [29]. Although *pkDAAO* adsorbs on both solid substrates even under unfavorable electrostatic conditions, the surface bio-activity is highly dependent on the ratio between τ_f and τ_{op} . The optimization step is electrostatic in nature on silica and hydrophobically driven on gold. Accordingly, the bio-activity of the native *pkDAAO* is preserved at any degree of surface coverage on silica whereas on gold it is only retained at high degree of surfaces coverage. However, these *pkDAAO* bio-functionalized gold platforms cannot be coupled to the commonly used amperometry technique because the analyte (D-alanine) interference increases the detection limit of the method. Consequently, different enzyme sources together with another adsorption strategy are required to improve the catalytic performance of DAAO bio-functionalized platforms.

This work is aimed at studying the adsorption process and surface bio-activity of His-tagged D-amino acid oxidase (DAAO) from *Rhodotorula gracilis* (*His₆-RgDAAO*) as the first step for the development of an electrochemical bio-functionalized platform. With such a purpose the bio-recognition element was expressed following the reported results by Pollegoni et al. [30,31] in order to determine the bio-activity of the native and adsorbed enzyme by amperometry and the adsorption mechanism on bare gold and carboxylated modified substrates in the absence (substrate/ COO^-) and presence of Ni(II) (substrate/ $\text{COO}^- + \text{Ni(II)}$) by reflectometry. Comparing the adsorption behavior and bio-activity of *His₆-RgDAAO* on these different solid substrates allows understanding the contribution of the diverse interactions responsible for the platform performance.

2. Experimental

2.1. Materials

All reagents were of analytical grade and were used without further purification: D-alanine (Fluka), H_2O_2 , KMnO_4 (Cicarelli), KH_2PO_4 , K_2HPO_4 , $\text{K}_4\text{P}_2\text{O}_7$, HClO_4 , NaOH , KClO_4 , and KOH (Baker), $\text{Na}_2\text{C}_2\text{O}_4$ (Riedel-de-Haën), KClO_4 (Erba), plasmid pET-15b (Novagen), isopropil- β -Dtiogalactósido (IPTG) (Biodynamics), and Ni(II)-nitrilotriacetic acid (Ni-NTA) agarose (Invitrogen). Aqueous solutions were prepared by using $18 \text{ M}\Omega \text{ cm}^{-1}$ resistance water (Milli-Q, Millipore; Billerica, MA). H_2O_2 concentration was determined by titration with 0.1 M KMnO_4 which was standardized against $\text{Na}_2\text{C}_2\text{O}_4$. 5 mM buffer solutions (PB) were prepared by dissolving the desired amount of KH_2PO_4 , K_2HPO_4 , $\text{K}_4\text{P}_2\text{O}_7$ in water and adjusting the pH with either 2 M KOH or 2 M HClO_4 to reach pH 5.0, 7.0, or 8.5. The pH measurements were performed with a combined glass electrode and a digital pH meter (Orion 420A+, Thermo; Waltham, MA, USA). Unless noted, all experiments were performed at room temperature ($26 \pm 2^\circ\text{C}$).

2.2. Cloning, expression, and purification of recombinant *His₆-RgDAAO*

The expression and purification of the recombinant *RgDAAO* engineered with a His₆-tag at the N-terminal of the enzyme were performed following the reported results by Pollegoni et al. [30–32]. The coding sequence of *RgDAAO* (EC 1.4.3.3, DAAO) was ordered from Genscript, with its codon usage optimized for *Escherichia coli* expression. The fragment was introduced by cloning into pET15b (NOVAGEN) which drives the expression of fusion proteins with a polihistidine tag at the N-terminus, to generate pJV398. This plasmid was transformed into *E. coli* BL21 strain for subsequent expression experiments. *Escherichia coli* cells were grown in LB medium (10 g L^{-1} tryptone, 5 g L^{-1} yeast extract, and 10 g L^{-1} NaCl) supplemented with 0.1% ampicillin and 0.5% glucose at 37°C with rotary shaking. When the cell optical density ($\text{OD} = 600$) reached 0.6, *His₆-RgDAAO* expression was induced with the addition of 1 mM IPTG for 3 h at 37°C . The bacterial pellet was resuspended in lysis buffer (15% glycerol, 0.5 M NaCl, 20 mM Tris-HCl pH 7.5) and the cells were lysed in an Emulsiflex High pressure homogenizer (AVESTIN). The homogenate was centrifuged at 10,000 rpm for 30 min. The supernatant containing recombinant *His₆-RgDAAO* was subject to purification by metal chelation chromatography using Ni(II)-NTA Agarose matrix (QUIAGEN). The protein bound to the resin was rinsed several times with imidazole gradient (20–200 mM). The imidazole was eliminated by gel filtration and the protein was eluted with water and then lyophilized. Purity was checked by SDS-PAGE followed by Coomassie staining.

2.3. Bio-functional platform

2.3.1. Solid substrates

As previously described [22], the surface properties of modified silica and gold solid substrates were proven to be indistinguishable [22]. The adsorption experiments were performed with silicon wafers (100 mm, Silicon Valley Microelectronics Inc.; Santa Clara, CA, USA) oxidized at 1000°C for 1 h (thickness was verified by ellipsometry) in order to obtain a silica layer of about 100 nm thick (essential for obtaining a high sensitivity in reflectometry experiments [33]) and cut in strips ($1 \text{ cm} \times 4 \text{ cm}$) following the crystallographic plane of silicon (100). Prior to each adsorption experiment, these strips were cleaned with boiling piranha solution (2:1 $\text{H}_2\text{SO}_4:\text{H}_2\text{O}_2$) and rinsed thoroughly with deionized water. (Caution! Piranha solution is a powerful oxidizing agent that reacts violently with organic compounds; it should be handled with extreme

care). Bio-activity in solution was determined using commercially available gold electrodes (CHI Instruments, Inc.) with a 0.12 cm² geometric surface area whereas the bio-functional platforms were prepared on gold strips (geometric surface area 1.5 cm²).

2.3.2. Modified solid substrates

Thermally oxidized silicon wafers were modified with a gold layer (gold) prepared by sputtering (SPI #12162-AB) the metal up to reaching a 10 nm layer (thickness was verified by ellipsometry) [29] and it did not substantially modify the optical behavior of the 100 nm SiO₂ layer [34]. Both oxidized silicon wafers and gold electrodes were modified following the previously described method [22] in order to have grafted carboxylate groups (substrate/COO⁻) or partially coordinated Ni(II) surface sites (substrate/COO⁻ + Ni(II)). This substrates modification produced two types of films: (a) a COO⁻ terminated self-assembled monolayer that formed a high affinity surface chelation complex with Ni(II) and (b) a polymeric glutaraldehyde film that physically incorporated Ni(II). This glutaraldehyde film did not affect the surface properties nor interfere with the electrochemical response of the substrate.

2.3.3. Bio-functionalized platform

Gold, substrate/COO⁻ and substrate/COO⁻ + Ni(II) were immersed in 0.1 mg mL⁻¹ His₆-RgDAAO solution at pH 8.5 during 1.5 h. Afterwards, the platforms were rinsed with PB and used as the working electrode of the electrochemical cell in order to amperometrically measure the H₂O₂ formation during the enzymatic reaction.

2.4. His₆-RgDAAO bio-activity

Amperometry measurements were carried out in a potentiostat CHI101 (CH Instruments, Inc.) with a three electrodes cell (25.0 mL for the bio-activity experiments with His₆-RgDAAO in solution and 8.5 mL for the bio-activity experiments with the bio-functional platforms) which containing a reference electrode (Ag/AgCl/KCl_{sat}) and platinum wire as counter electrode. The working electrode was either gold or the bio-functional platform (adsorbed His₆-RgDAAO on substrate/COO⁻ or substrate/COO⁻ + Ni(II)) to determine the bio-activity in solution or on the surface, respectively. Bio-activity experiments were carried out by using the batch amperometric method to measure the H₂O₂ concentration produced by the enzymatic reaction, applying a potential (H₂O₂ oxidation) of 450 mV (pH 8.5), 550 mV (pH 7.0), or 650 mV (pH 5.0) [29].

The experiments performed to determine the bio-activity in solution started with a stirred D-alanine solution (the enzyme substrate) ranging between 0.1 mM and 3.0 mM prepared in PB to record the baseline and the further addition of the enzyme at different concentrations (0.1–2.5 μg mL⁻¹ range). In the presence of His₆-RgDAAO, the current intensity increased due to the H₂O₂ production which allows determining the initial enzymatic reaction rate (*V*₀) in real-time experiments. Calibration curves (as an example see Fig. 1 in Supplementary information) were performed in exactly the same electrochemical cell in the absence of His₆-RgDAAO before and after each bio-activity experiment to check the reproducibility and the electrode stability. The calibration curves were determined following the amperometric response on the bare gold electrode for successive additions of H₂O₂ (previously titrated with standardized KMnO₄) to the electrochemical cell. Considering that the quantity of produced H₂O₂ during the enzymatic reaction changed in a wide concentration range (depending on the enzyme concentration and pH), the added volume and concentration of H₂O₂ were selected to be as close as possible to the enzymatic reaction.

Surface bio-activity was measured by adding D-alanine (0.1 mM and 3.0 mM) to a stirred PB (pH 8.5) solution and allowing the transient current to reach a steady-state value. Due to the small amount of the enzyme on the platforms, the addition of D-alanine during the experiments caused a change in the current intensity. However, this interference was constant for all the studied concentrations and negligible at H₂O₂ concentrations higher than 1 μM. Nevertheless, it was subtracted from the calibration curves to calculate the actual H₂O₂ concentration produced during the enzymatic reaction. The calibration curves and the analytical parameters to quantify H₂O₂ concentration are given as supplementary information. Calibration curves were performed in exactly the same electrochemical cell in the absence of D-alanine before and after each bio-activity experiment to check the reproducibility and the electrode stability. The calibration curves were determined following the amperometric response on the bio-functional platform (adsorbed His₆-RgDAAO on substrate/COO⁻ or substrate/COO⁻ + Ni(II)) for successive addition of H₂O₂ (previously titrated with standardized KMnO₄) to the electrochemical cell. Due to the different working electrodes (either gold or the bio-functional platforms) the sensitivity towards H₂O₂ determination diminished (see supplementary information) when using the modified substrates in the presence of the adsorbed enzyme.

The experiments were performed in triplicate and the average results plot as *V*₀ vs. D-alanine concentration. The standard deviations of these three measurements were used to calculate the error bars. The enzyme kinetics curves at the different His₆-RgDAAO concentrations (both in solution and on the surface) were fitted with non-linear regression routines to calculate the relevant parameters.

To check the stability of the bio-functionalized platforms (prepared as it was indicated in Section 2.3.3), the H₂O₂ concentration produced by the enzymatic reaction (0.1 mg mL⁻¹ His₆-RgDAAO initial concentration) in the presence of 1 mM D-alanine was determined before and after washing with unspecific (200 mM KNO₃) or specific (200 mM histidine) agents.

2.5. His₆-RgDAAO adsorption mechanism

Real-time adsorption–desorption experiments were performed in a reflectometer (AKZO Research Laboratories, Arnhem), equipped with a stagnation point flow cell as described elsewhere [35,36]. Briefly, from 0 s to 200 s, only PB was introduced into the cell and a stable baseline was obtained. Then (from 200 s to 2700 s), the flow was switched from PB to a His₆-RgDAAO solution. Next (between 2700 s and 3500 s), the flow was switched back to the initial PB in order to analyze the desorption process by dilution. The adsorption–desorption experiments were conducted with His₆-RgDAAO at different concentrations (ranging from 0.001 mg mL⁻¹ to 0.100 mg mL⁻¹) at pH 8.5.

As described in [37], to calculate the sensitivity factor (*Q*-factor) that provides the proportionality constant between the measured signal and the adsorbed amount (*I*), the substrate was modeled as a Si substrate (refraction index of 3.80) with a 100 nm SiO₂ layer (refraction index of 1.46) and a 10 nm Au layer (refraction index of 0.10) immersed in aqueous solution (refraction index of 1.333) and the increment in the refraction index with the protein concentration (dn/dc) was considered to be 0.18 [38]. The calculated *Q*-factors resulted in 30 ± 5 mg m⁻² and 110 ± 5 mg m⁻² for silica and gold substrates, respectively.

To study the different steps involved in the overall protein adsorption process, the experimental kinetics curves were normalized by the supply rate (*t* × *C*_p, see Supplementary information, Fig. 2) to account for the actual effect of the protein concentration on the adsorption mechanism. Since these normalized kinetics curves did not merge (especially at low protein concentrations) there were two competitive processes occurring in the same time scale [39].

Considering that the protein transport toward the substrate was well controlled by the stagnation point flow of the reflectometer setup, the transport constant ($k_{tr} = 5 \times 10^{-6} \text{ m s}^{-1}$) was calculated [40] from the linear relationship between the supply rate and the protein concentration in solution. Further, the adsorption kinetic constants ($k_{ads} = (3 \pm 1) \times 10^{-6} \text{ m s}^{-1}$ for the three solid substrates) were calculated from the slope of the linear plot of the initial adsorption rate (v_{ads}) as a function of the protein concentration (Supplementary information, Fig. 3).

3. Results and discussion

3.1. His₆-RgDAAO bio-activity in solution

Fig. 1A compares the current intensity vs. time profiles due to the H₂O₂ produced during the enzymatic reaction to oxidize D-alanine to the corresponding α -keto acids in the presence of either His₆-RgDAAO or *pk*DAAO in solution. The ammonia produced during the enzymatic reaction did not interfere with the electrochemical determination. Two important features appeared from these results: (1) the current intensity was higher with the recombinant His₆-RgDAAO, (2) H₂O₂ production with the recombinant enzyme was so high that the steady-state values between successive additions of D-alanine were not reached in the course of the experiment. In the first place, the enzymatic activity of His₆-RgDAAO was 10 times higher than that of *pk*DAAO, indicating that lower D-alanine concentrations can be determined with the recombinant enzyme. Secondly, the kinetic parameters to describe the His₆-RgDAAO behavior in solution could be determined from the initial enzymatic reaction rate (V_0) measured in real-time amperometry experiments.

Fig. 1B shows the current intensity vs. time profile at short reaction times together with the linear fitting needed to calculate V_0 for the enzymatic reaction of His₆-RgDAAO in solution. From these measurements the classical V_0 vs. D-alanine concentration plots (Fig. 2A) were generated in order to determine the kinetic parameters that characterize His₆-RgDAAO bio-activity in solution. The maximum enzymatic reaction rate (V_{max}) and the Michaelis constant (K_M) were calculated from non-linear regression of the experimental data measured at different His₆-RgDAAO

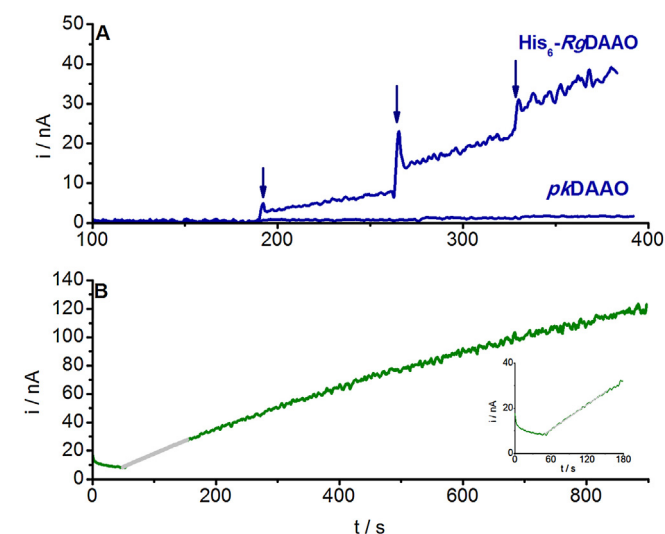


Fig. 1. Bio-activity of DAAO in PB at pH 8.5 as measured by amperometry: current intensity (i) vs. time (t) profile. (A) For successive addition (0.1 mmol) of D-alanine (indicated by the arrows) to either His₆-RgDAAO or *pk*DAAO of the same concentration (10.0 $\mu\text{g mL}^{-1}$). (B) For the addition of 0.1 $\mu\text{g mL}^{-1}$ His₆-RgDAAO to 2.0 mM D-alanine solution. Applied potential: 450 mV vs. Ag/AgCl/KCl_{sat}. Working electrode: bare gold. Counter electrode: Pt wire.

concentrations. Fig. 2B shows V_{max} and K_M as a function of His₆-RgDAAO concentration at pH 8.5. As expected from the simple Michaelis–Menten model [41], V_{max} was directly proportional to the enzyme concentration and K_M remained almost invariant (within experimental error) with the enzyme concentration (0.4 mM). Under the same experimental conditions, the K_M value of *pk*DAAO was higher (5 mM) [29,42]. At pH 7.0 (data not shown), K_M values were of the same order (0.4 ± 0.2) while V_{max} (9 ± 2) was one order of magnitude lower when the same His₆-RgDAAO concentration (2.5 $\mu\text{g mL}^{-1}$) was used. Finally, at pH 5.0 (data not shown) both K_M (3 ± 1 mM) and V_{max} ($1.4 \pm 0.1 \mu\text{M min}^{-1}$) values were different. This behavior agrees with reported results showing that D-amino acids with deprotonated amino groups are the best substrates for DAAO [4,43] and that pH 8.5 is optimum to measure DAAO enzymatic activity. It is important to note that the highly improved enzymatic performance of His₆-RgDAAO (compared to *pk*DAAO [29]) indicates that the recombinant enzyme is a viable bio-recognition element of D-amino acids to be coupled to electrochemical platforms.

3.2. His₆-RgDAAO adsorption mechanism

Real-time adsorption–desorption kinetic profiles were measured by reflectometry at pH 8.5 on the three solid substrates (Supplementary information, Fig. 2): gold, substrate/COO[−] and substrate/COO[−] + Ni(II). The adsorption of His₆-RgDAAO was induced at pH 8.5 to favor surface bio-activity, promote the bio-affinity interaction between the His-tag and the Ni(II) surface sites while minimizing electrostatic interactions between the enzyme and the bare sorbent substrate [21]. However, physical adsorption could not be completely removed even under these unfavorable conditions. Therefore, the experiments conducted on either gold or substrate/COO[−] allowed determining the extent of the physical adsorption, mostly driven by electrostatic and hydrophobic interactions. At pH 8.5, COO[−] surface groups were deprotonated as well as the protein lateral chains, diminishing the possibility of hydrogen bond formation.

The adsorption kinetic constants ($k_{ads} = (3 \pm 1) \times 10^{-6} \text{ m s}^{-1}$) were not significantly different than k_{tr} ($5 \times 10^{-6} \text{ m s}^{-1}$) indicating that the adsorption process of His₆-RgDAAO was transport-controlled both in the absence (physical adsorption) and presence (bio-affinity interactions) of Ni(II) sites. This behavior was already measured for physically adsorbed *pk*DAAO ($k_{ads} = (2 \pm 1) \times 10^{-6} \text{ m s}^{-1}$) [29] and it has been attributed to the primary structure of the enzyme with positively charged side chains even at pH 8.5. The transport-controlled adsorption of DAAO indicated that the first contact between the enzyme and the solid substrate was ruled by electrostatic interactions, in line with the first stage of the adsorption mechanism of the His-tag antigen on Ni(II) modified substrate [21]. Also in this case, there were two competitive processes occurring in the same time scale indicating the presence of a second step (following the first electrostatic interaction), related to either the surface bio-affinity interaction or any other process. This optimization process was evaluated from the relationship between τ_f and τ_{op} [21,29]. When the adsorption process is transport-controlled, τ_f can be calculated as the ratio between the saturation adsorbed amount and the initial adsorption rate (Supplementary information, Figs. 4 and 5). On the other hand, τ_{op} (around 10^2 s) was estimated by extrapolating to zero Γ_{sat} (Supplementary information, Fig. 5).

Fig. 3 shows the dependence of the ratio τ_f/τ_{op} on the degree of surface coverage (expressed as the ratio between the saturation adsorbed amount, Γ_{sat} , and the maximum adsorbed amount, Γ_{max}) on the three solid substrates. The ratio between τ_f and τ_{op} depended on the degree of surface coverage, approaching 1

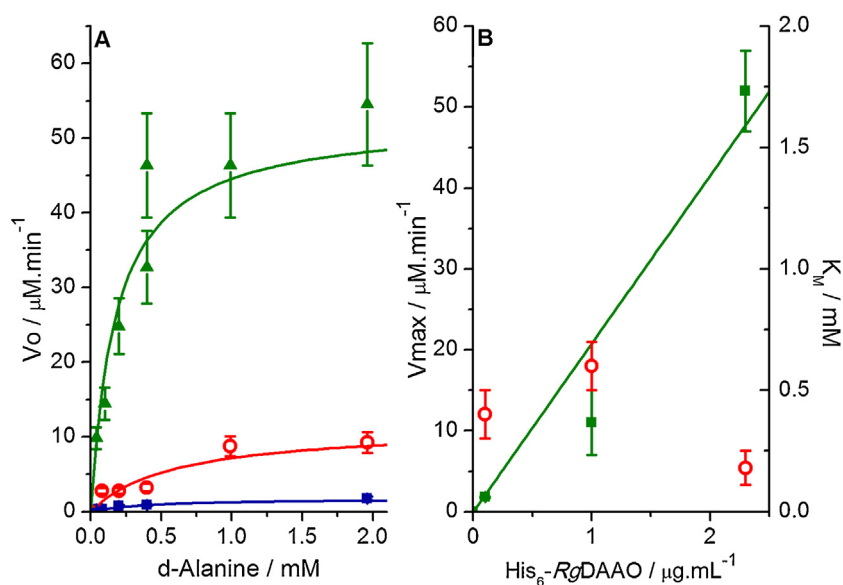


Fig. 2. (A) Initial enzymatic reaction rate (V_0) as a function of D-alanine concentration of the enzyme in solution at pH 8.5 and three His₆-RgDAAO concentrations: (■) 0.1 $\mu\text{g}\cdot\text{mL}^{-1}$, (○), 1.0 $\mu\text{g}\cdot\text{mL}^{-1}$, and (▲) 2.5 $\mu\text{g}\cdot\text{mL}^{-1}$. Lines were calculated from non-linear regression fittings using the Michaelis–Menten equation. (B) Kinetic parameters of His₆-RgDAAO in solution: (left axis) Maximum enzymatic reaction rate (V_{max}) and (right axis) Michaelis constant (K_M) as a function of His₆-RgDAAO concentration in PB at pH 8.5 determined from the non-linear regression fittings. Error bars denote standard deviations of three repeats. Applied potential: 450 mV vs. Ag/AgCl/KCl_{sat}. Working electrode: bare gold. Counter electrode: Pt wire.

at low surface coverage. At very low surface coverage, the optimization process may be faster than filling the surface (i.e. every attached enzyme optimized its interaction with the surface when it had enough space). Neither the ratio τ_f/τ_{op} nor its dependence with the degree of surface coverage depended on the nature of the solid substrate (i.e. bio-affinity interactions if any could not be confirmed by these experiments). Moreover, desorption experiments (upon adding buffer) did not show any dependence either (data not shown). Consequently, surface bio-activity experiments were performed before and after washing with different agents to get a deeper insight into the interactions that were involved in the adsorption mechanism.

Fig. 4 compares the enzymatic activity of the His₆-RgDAAO platforms before (indicated as 100%) and after washing with 200 mM KNO₃ or 200 mM histidine solution (expressed as the remaining

activity). The first one represents an unspecific agent that can remove electrostatically adsorbed enzymes while the other one directly competes with the His-tag protein for the Ni(II) surface sites [21]. In the absence of Ni(II), the surface bio-activity diminished to the same extent with both washing agents (around 30% on gold and 15% on substrate/COO⁻). As expected, the desorption mechanism did not depend on the specificity of the washing toward Ni(II)–histidine interactions. However, these experiments clearly showed that the interaction of His₆-RgDAAO with the sorbent substrate was stronger in the presence of surface COO⁻ because the washing treatments removed only a small portion of the active enzymes. On the other hand, there was a strong effect in the presence of Ni(II) surface sites: the surface bio-activity diminished around 15% when using 200 mM KNO₃ whereas more than 80% was lost after using the competitive agent. Consequently, the surface bio-activity of the bio-functionalized platforms in the presence of Ni(II) was mainly provided from His₆-RgDAAO attached to the

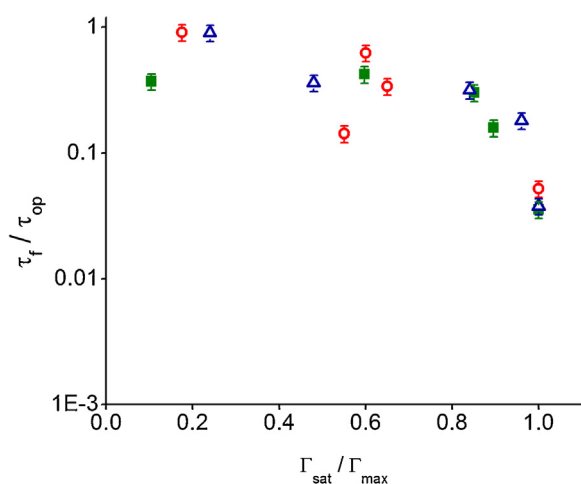


Fig. 3. The ratio between the filling (τ_f) and optimization (τ_{op}) times as a function of the degree of surface coverage ($\Gamma_{\text{sat}}/\Gamma_{\text{max}}$) of His₆-RgDAAO adsorbed on (■) bare gold and COO⁻ modified substrates in the (○) absence (substrate/COO⁻) and (△) presence (substrate/COO⁻ + Ni(II)) of Ni(II) surface sites at pH 8.5. Error bars denote standard deviations of three repeats.

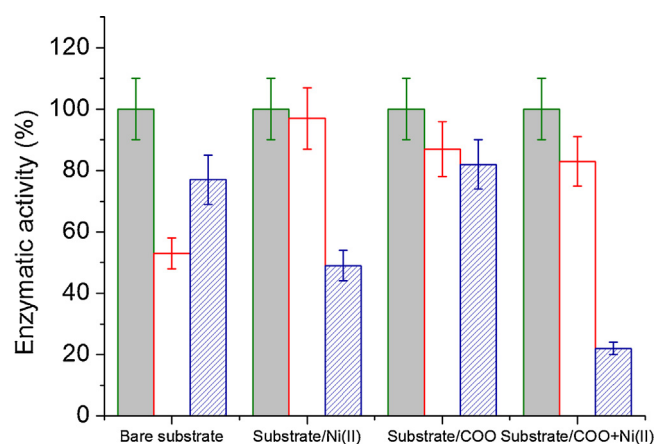


Fig. 4. Enzymatic activity (in the presence of 1.0 mM D-alanine) of His₆-RgDAAO adsorbed on bare gold, substrate/COO⁻ and substrate/COO⁻ + Ni(II) at pH 8.5 (solid, 100%) before and after washing with (open) 200 mM KNO₃ or (pattern) 200 mM histidine solutions. Ni(II) modified gold substrates are also included for comparison purposes. Error bars denote standard deviations of three repeats.

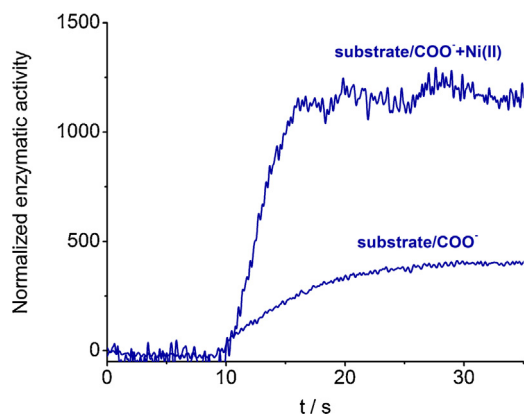


Fig. 5. Normalized enzymatic activity as a function of time (t) measured with the bio-functional platforms (adsorbed His₆-RgDAAO on substrate/COO⁻ or substrate/COO⁻ + Ni(II)) at pH 8.5. Enzymatic activity was determined amperometrically in the presence of 0.1 mM D-alanine and normalized by the mass of adsorbed His₆-RgDAAO on each substrate as measured by reflectometry. Applied Potential: 450 mV vs. Ag/AgCl/KCl_{sat}. Working electrode: bio-functional platforms. Counter electrode: Pt wire.

sorbent substrate through bio-affinity interactions. As a proof of concept, Fig. 4 also includes the performance of a His₆-RgDAAO bio-functionalized platforms prepared on gold substrate modified with Ni(II) by the direct dipping in a Ni(NO₃)₂ aqueous solution. There was also a clear effect of the competitive agent on the surface bio-activity but it was to a lower extent (around 50% of the surface bio-activity remained after washing with the histidine solution). As recently reported with different proteins and cations [9], metal activated surfaces enhance the strength of the interaction by orders of magnitude.

It is interesting to note that electrostatic interactions play a major role in the adsorption mechanism of His₆-RgDAAO on either bare or modified substrates. Moreover, they cannot be completely removed even after these washing treatments. The presence of Ni(II) on gold favors these interactions resulting in a rather inefficient washing with KNO₃ whereas COO⁻ modified substrates, which are more hydrophobic than the bare gold [22], respond weakly to both treatments. In view of these results, the optimization step in the absence of Ni(II) surface sites may be related to some degree of spreading of the adsorbed enzymes. This effect may be more evident at low degree of surface coverage when $\tau_f \sim \tau_{op}$. On the other hand, the optimization step is caused by the bio-affinity interaction between the His-tag of the enzyme and the Ni(II) surface sites. This step also depends on the degree of surface coverage: At low degree of surface coverage, His₆-RgDAAO molecules has time and space to achieve the proper orientation for the bio-affinity interaction ($\tau_f \sim \tau_{op}$) whereas the orientation restriction caused by the small size of the tag compared to the whole enzyme is more marked ($\tau_f < \tau_{op}$) at high degree of surface coverage. Consequently, in these cases the ratio τ_f/τ_{op} as a function of the degree of surface coverage does not depend on the interactions that control the adsorption mechanism. Finally, these results also indicate that the His₆-RgDAAO bio-functionalized platform in the presence of Ni(II) surface sites is stable against unspecific washings and re-usable after using competitive agents.

3.3. His₆-RgDAAO bio-activity of bio-functionalized platforms

Fig. 5 shows the normalized enzymatic activity of the bio-functional platforms at pH 8.5 as a function of time using just one D-alanine concentration (0.10 mM). The activity was determined from the H₂O₂ concentration produced by the enzymatic reaction normalized by the mass of adsorbed His₆-RgDAAO on

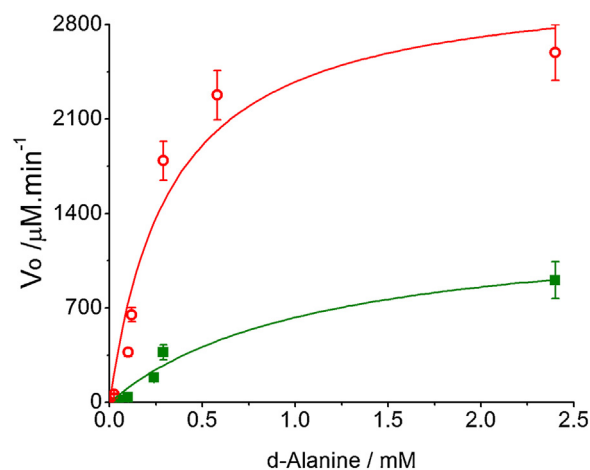


Fig. 6. Initial enzymatic reaction rate (V_o) as a function of D-alanine concentration of the bio-functional platforms prepared on (■) substrate/COO⁻ and (○) substrate/COO⁻ + Ni(II) at pH 8.5. Lines were calculated from non-linear regression fittings using the Michaelis–Menten equation. Error bars denote standard deviations of three repeats. Applied potential: 450 mV vs. Ag/AgCl/KCl_{sat}. Working electrode: bio-functional platform. Counter electrode: Pt wire.

Table 1

Maximum enzymatic reaction rate (V_{max}), Michaelis constant (K_M) and catalytic constant (k_{cat}) for the enzymatic reaction of His₆-RgDAAO in solution and adsorbed on COO⁻ modified substrates in the absence and presence of Ni(II) surface sites at pH 8.5.

His ₆ -RgDAAO	K_M (mM)	V_{max} ($\mu\text{M min}^{-1}$)	k_{cat} (min^{-1})
COO ⁻ modified substrate	0.5 ± 0.1	$(1.2 \pm 0.2) \times 10^3$	4×10^6
COO ⁻ modified substrate + Ni(II)	0.2 ± 0.1	$(3.1 \pm 0.5) \times 10^3$	7×10^6
Solution ($0.1 \mu\text{g mL}^{-1}$)	0.2 ± 0.1	1.8 ± 0.1	2×10^4

substrate/COO⁻ (0.20 μg) or substrate/COO⁻ + Ni(II) (0.25 μg), as measured by reflectometry. This figure clearly indicates the better performance of the His₆-RgDAAO bio-functionalized platform in the presence of Ni(II) surface sites (i.e. when the bio-affinity interaction became possible). Performing the same experiment as a function of the enzyme substrate, allowed generating the classical V_o vs. D-alanine concentration curves shown in Fig. 6. Table 1 compares the Michaelis–Menten parameters as well as the turnover rate (k_{cat}) of the enzyme in solution ($0.1 \mu\text{g mL}^{-1}$) to the His₆-RgDAAO bio-functionalized platforms in the absence and presence of Ni(II) surface sites.

K_M values indicated that the adsorbed enzyme on COO⁻ modified substrate had a lower affinity for D-alanine than the native His₆-RgDAAO. Consequently, the enzyme conformation was partially perturbed during the optimization step altering its bio-recognition capabilities. However, K_M did not change (within experimental error) when the bio-affinity interactions were feasible, pointing to native-like molecules on the platform. On the other hand, both V_{max} and k_{cat} showed a better catalytic efficiency of the enzyme on both platforms than in solution. However, the reasons behind these behaviors may be different. With physically adsorbed enzymes, an increased catalytic activity has been assigned to the exposure of the active site due to conformational changes caused by the sorbent substrate [11,44]. Considering that DAAO is a FAD-dependent flavoenzyme, the surface perturbation may affect the protein conformation in the same direction as observed with cytochrome c adsorbed on graphene oxide, which also exhibits an exceptionally high activity because of the exposure of the heme group [11]. On the other hand, some enzymes confined on mesoporous materials by covalent or bio-affinity interactions show similar or better catalytic behavior than in solution together with an increased stability against pH and temperature

[45–48]. This improved enzymatic response has been assigned to the chain compaction of entrapped enzymes. Further, the enhanced stability has also been observed with RgDAAO with C-terminal His-tags adsorbed on porous supports whereas the catalytic efficiency is lower than in solution due to multipoint attachment [24]. COO⁻ terminated self-assembled monolayers [22] together with histidine–Ni(II) interactions may also promote chain compaction resulting in an ordered layer of oriented protein molecules. Therefore, the enhanced bio-activity observed with His₆-RgDAAO bio-functionalized platforms in the presence of Ni(II) sites may be due to ordered adsorbed enzymes that retain their native structure and maintain a proper orientation on the surface. Finally, it is important to emphasize that His₆-RgDAAO bio-functionalized platforms exhibits a higher surface activity than pkDAAO physically adsorbed on gold [29]. This behavior is due to the better performance of the first enzyme as recognition element as well as the improved quality of the bio-functionalization strategy based on the bio-affinity interactions between Ni(II) surface sites and the histidine residues of the protein.

4. Conclusions

His₆-RgDAAO bio-functionalized platforms built on solid substrates modified with carboxylate terminated self-assembled monolayers in the presence of Ni(II) surface sites present enhanced bio-activity because the surface complexes histidine–Ni(II) provide with site-oriented, native-like enzymes. The adsorption mechanism responsible of the excellent performance of the bio-functionalized platform takes place in two steps involving electrostatic and bio-affinity interactions whose prevalence depends on the degree of surface coverage.

The assembled bio-functionalized platform can be prepared on flat substrates or (nano)particles to be used in biosensing, drug delivery, and decontamination systems using different His-tagged proteins due to its highly bio-activity, stability, and re-usability properties.

Acknowledgments

The authors acknowledge ANPCyT, SeCyT-UNC, and CONICET for financial support. EH thanks CONICET for fellowships.

Appendix A. Supplementary data

Supplementary data associated with this article can be found, in the online version, at <http://dx.doi.org/10.1016/j.apsusc.2015.08.121>.

References

- [1] Y. Li, L. Fang, P. Cheng, J. Deng, L. Jiang, H. Huang, et al., An electrochemical immunosensor for sensitive detection of *Escherichia coli* O157:H7 using C60 based biocompatible platform and enzyme functionalized Pt nanochains tracing tag, *Biosens. Bioelectron.* 49 (2013) 485–491, <http://dx.doi.org/10.1016/j.bios.2013.06.008>.
- [2] R. Fogel, J.L. Limson, Probing fundamental film parameters of immobilized enzymes – Towards enhanced biosensor performance. Part II – Electroanalytical estimation of immobilized enzyme performance, *Enzyme Microb. Technol.* 49 (2011) 153–159, <http://dx.doi.org/10.1016/j.enzmictec.2011.05.004>.
- [3] M.L. Mena, P. Yáñez-Sedeño, J.M. Pingarrón, A comparison of different strategies for the construction of amperometric enzyme biosensors using gold nanoparticle-modified electrodes, *Anal. Biochem.* 336 (2005) 20–27, <http://dx.doi.org/10.1016/j.ab.2004.07.038>.
- [4] L.E. Valenti, E. Herrera, F. Stragliotto, V.L. Martins, R.M. Torresi, C.E. Giacomelli, et al., Optimizing the bioaffinity interaction between His-Tag proteins and Ni(II) surface sites, in: *ACS Proteins Interfaces III*, ACS Symposium Series, 2012, pp. 37–53 (Chapter 2).
- [5] C.E. Giacomelli, L.E. Valenti, L. Carot, Biomolecules and solid substrate interaction: Key factors in developing biofunctional surfaces *Encyclopedia of Surface and Colloid Science*, Second Edition, Taylor & Francis, 2007, pp. 1–16, <http://dx.doi.org/10.1081/E-ESCS-120047144>.
- [6] S.N. Jamadagni, R. Godawat, S. Garde, Hydrophobicity of proteins and interfaces: Insights from density fluctuations, *Annu. Rev. Chem. Biomol. Eng.* 2 (2011) 147–171, <http://dx.doi.org/10.1146/annurev-chembioeng-061010-114156>.
- [7] C.E. Giacomelli, W. Norde, Influence of hydrophobic teflon particles on the structure of amyloid beta-peptide, *Biomacromolecules* 4 (2003) 1719–1726, <http://dx.doi.org/10.1021/bm034151g>.
- [8] M.F. Mora, C.E. Giacomelli, C.D. Garcia, Interaction of D-amino acid oxidase with carbon nanotubes: Implications in the design of biosensors, *Anal. Chem.* 81 (2009) 1016–1022, <http://dx.doi.org/10.1021/ac802068n>.
- [9] A. Pattammattel, I.K. Deshapriya, R. Chowdhury, C.V. Kumar, Metal-enzyme frameworks: Role of metal ions in promoting enzyme self-assembly on α-zirconium(IV) phosphate nanoplates, *Langmuir* 29 (2013) 2971–2981, <http://dx.doi.org/10.1021/la304979s>.
- [10] X. Liu, X. Chen, Y. Li, X. Wang, X. Peng, W. Zhu, Preparation of superparamagnetic Fe₃O₄@alginate/chitosan nanospheres for candida rugosa lipase immobilization and utilization of layer-by-layer assembly to enhance the stability of immobilized lipase, *ACS Appl. Mater. Interfaces* (2012), <http://dx.doi.org/10.1021/am301104c>.
- [11] A. Pattammattel, M. Puglia, S. Chakraborty, I.K. Deshapriya, P.K. Dutta, C.V. Kumar, Tuning the activities and structures of enzymes bound to graphene oxide with a protein glue, *Langmuir* (2013), <http://dx.doi.org/10.1021/la404051c>.
- [12] A.S. Campbell, C. Dong, F. Meng, J. Hardinger, G. Perhinschi, N. Wu, et al., Enzyme catalytic efficiency: A function of bio-nano interface reactions, *ACS Appl. Mater. Interfaces* 6 (2014) 5393–5403.
- [13] V. Bille, D. Plainchamp, S. Lavielle, G. Chassaing, J. Remacle, Effect of the microenvironment on the kinetic properties of immobilized enzymes, *Eur. J. Biochem.* 180 (1989) 41–47.
- [14] U. Guzik, K. Hupert-Kocurek, D. Wojcieszynska, Immobilization as a strategy for improving enzyme properties—application to oxidoreductases, *Molecules* 19 (2014) 8995–9018, <http://dx.doi.org/10.3390/molecules19078995>.
- [15] W. Tischer, F. Wedekind, Immobilized enzymes: Methods and applications, *Current* 200 (1999) 95–126, http://dx.doi.org/10.1007/3-540-68116-7_4.
- [16] L.E. Valenti, C.P. De Pauli, C.E. Giacomelli, The binding of Ni(II) ions to hexahistidine as a model system of the interaction between nickel and His-tagged proteins, *J. Inorg. Biochem.* 100 (2006) 192–200, <http://dx.doi.org/10.1016/j.jinorgbio.2005.11.003>.
- [17] L. Nieba, S.E. Nieba-Axmann, A. Persson, M. Hämäläinen, F. Edebratt, A. Hansson, et al., BIACORE analysis of histidine-tagged proteins using a chelating NTA sensor chip, *Anal. Biochem.* 252 (1997) 217–228, <http://dx.doi.org/10.1006/abio.1997.2326>.
- [18] M. Fischer, A.P. Leech, R.E. Hubbard, Comparative assessment of different histidine-tags for immobilization of protein onto surface plasmon resonance sensorchips, *Anal. Chem.* 83 (2011) 1800–1807, <http://dx.doi.org/10.1021/ac103168q>.
- [19] P.A. Millner, H.C.W. Hays, A. Vakurov, N.A. Pchelintsev, M.M. Billah, M.A. Rodgers, Nanostructured transducer surfaces for electrochemical biosensor construction – Interfacing the sensing component with the electrode, *Semin. Cell Dev. Biol.* 20 (2009) 34–40, <http://dx.doi.org/10.1016/j.semcdb.2009.01.011>.
- [20] C. Smith, S.M. Giang, No title, *Top Curr. Chem.* 261 (2010) 63.
- [21] L.E. Valenti, A.M. Smania, C.P. De Pauli, C.E. Giacomelli, Driving forces for the adsorption of a His-tag Chagas antigen. A rational approach to design bio-functional surfaces, *Colloids Surf. B Biointerfaces* 112 (2013) 294–301, <http://dx.doi.org/10.1016/j.colsurfb.2013.07.059>.
- [22] L.E. Valenti, V.L. Martins, E. Herrera, R.M. Torresi, C.E. Giacomelli, Ni(II)-modified solid substrates as a platform to adsorb His-tag proteins, *J. Mater. Chem. B* 1 (2013) 4921, <http://dx.doi.org/10.1039/c3tb20769b>.
- [23] J. Hou, Q. Jin, J. Du, Q. Li, Q. Yuan, J. Yang, A rapid in situ immobilization of D-amino acid oxidase based on immobilized metal affinity chromatography, *Bioprocess Biosyst. Eng.* 37 (2014) 857–864, <http://dx.doi.org/10.1007/s00449-013-1056-6>.
- [24] I. Kuan, R. Liao, H. Hsieh, K. Chen, C. Yu, Properties of rhodotorula gracilis D-amino acid oxidase immobilized on magnetic beads through his-tag, *J. Biosci. Bioeng.* 105 (2008) 110–115, <http://dx.doi.org/10.1263/jbb.105.110>.
- [25] A. Bava, D-amino acid oxidase – Nanoparticle system: A potential novel approach for cancer enzymatic therapy R research Article, *Nanomedicine* 8 (2013) 1797–1806.
- [26] H. Zheng, X. Wang, J. Chen, K. Zhu, Y. Zhao, Y. Yang, et al., Expression, purification, and immobilization of His-tagged D-amino acid oxidase of *Trigonopsis variabilis* in *Pichia pastoris*, *Appl. Microbiol. Biotechnol.* 70 (2006) 683–689, <http://dx.doi.org/10.1007/s00253-005-0158-8>.
- [27] X. Wu, B.J. Van Wie, D.A. Kidwell, An enzyme electrode for amperometric measurement of D-amino acid, *Biosens. Bioelectron.* 20 (2004) 879–886, <http://dx.doi.org/10.1016/j.bios.2004.04.002>.
- [28] M. Wcislo, D. Compagnone, M. Trojanowicz, Enantioselective screen-printed amperometric biosensor for the determination of D-amino acids, *Bioelectrochemistry* 71 (2007) 91–98, <http://dx.doi.org/10.1016/j.bioelectrochem.2006.09.001>.

- [29] E. Herrera, C.E. Giacomelli, Surface coverage dictates the surface bio-activity of D-amino acid oxidase, *Colloids Surf. B Biointerfaces* 117C (2014) 296–302, <http://dx.doi.org/10.1016/j.colsurfb.2014.02.050>.
- [30] L. Pollegioni, G. Molla, S. Campaner, E. Martegani, M.S. Pilone, Cloning, sequencing and expression in *E. coli* of a D-amino acid oxidase cDNA from *Rhodotorula gracilis* active on cephalosporin C, *J. Biotechnol.* 58 (1997) 115–123, <http://www.ncbi.nlm.nih.gov/pubmed/9383984>.
- [31] G. Molla, C. Vegezzi, M.S. Pilone, L. Pollegioni, Overexpression in *Escherichia coli* of a recombinant chimeric *Rhodotorula gracilis* D-amino acid oxidase, *Protein Exp. Purif.* 14 (1998) 289–294.
- [32] Qiagen, The QIAexpressionist, 2003, <http://scholar.google.com/scholar?hl=en&btnG=Search&q=intitle:The+QIAexpressionist+?#0>.
- [33] J.C. Dijt, M.A.C. Stuart, G.J. Fleer, Reflectometry as a tool for adsorption studies, *Adv. Colloid Interface Sci.* 50 (1994) 79–101.
- [34] T. Roques-Carmes, F. Membrey, C. Filiâtre, a. Foissy, Potentiality of reflectometry for the study of the adsorption on dielectric and metal substrates: Application to the adsorption of polyvinylimidazole on silica and gold, *J. Colloid Interface Sci.* 245 (2002) 257–266, <http://dx.doi.org/10.1006/jcis.2001.8007>.
- [35] J.C. Dijt, M.A.C. Stuart, J.E. Hofmann, G.J. Fleer, Kinetics of polymer adsorption in stagnation point flow, *Cell* 51 (1990) 141–158.
- [36] L.E. Valenti, P.A. Fiorito, C.D. García, C.E. Giacomelli, The adsorption–desorption process of bovine serum albumin on carbon nanotubes, *J. Colloid Interface Sci.* 307 (2007) 349–356, <http://dx.doi.org/10.1016/j.jcis.2006.11.046>.
- [37] N.G. Hoogeveen, M. Cohen Stuart, G.J. Fleer, Polyelectrolyte adsorption on oxides, *J. Colloid Interface Sci.* 145 (1996) 133–145.
- [38] C.E. Giacomelli, M. Esplandiú, P. Ortiz, M. Avena, C.P. De Pauli, Ellipsometric study of bovine serum albumin adsorbed onto Ti/TiO₂ electrodes, *J. Colloid Interface Sci.* 218 (1999) 404–411, <http://dx.doi.org/10.1006/jcis.1999.6434>.
- [39] C.F. Wertz, M.M. Santore, Effect of surface hydrophobicity on adsorption and relaxation kinetics of albumin and fibrinogen: Single-species and competitive behavior, *Langmuir* 17 (2001) 3006–3016.
- [40] T. Dabroś, T.G.M. Ven, A direct method for studying particle deposition onto solid surfaces, *Colloid Polym. Sci.* 261 (1983) 694–707, <http://dx.doi.org/10.1007/BF01415042>.
- [41] A.G. Marangoni, *Enzyme Kinetics. A Modern Approach*, Wiley Interscience, New York, 2003, Chapter 3, pp 44–60. ISBN: 978-0-471-15985-8.
- [42] V.I. Tishkov, S.V. Khoronenkova, Amino acid oxidase: Structure, catalytic mechanism, and practical application, *Biochemistry (Mosc.)* 70 (2005) 40–54.
- [43] M.A. Vanoni, A. Cosma, D. Mazzeo, A. Mattevi, F. Todone, B. Curti, Limited proteolysis and X-ray crystallography reveal the origin of substrate specificity and of the rate-limiting product release during oxidation of D-amino acids catalyzed by mammalian D-amino acid oxidase, *Biochemistry* 36 (1997) 5624–5632, <http://dx.doi.org/10.1021/bi963023s>.
- [44] S. Wang, Y. Zhang, N. Abidi, L. Cabrales, Wettability and surface free energy of graphene films, *Langmuir* 25 (2009) 11078–11081, <http://dx.doi.org/10.1021/la901402f>.
- [45] C.-H. Lee, T.-S. Lin, C.-Y. Mou, Mesoporous materials for encapsulating enzymes, *Nano Today* 4 (2009) 165–179, <http://dx.doi.org/10.1016/j.nantod.2009.02.001>.
- [46] N. Carlsson, H. Gustafsson, C. Thörn, L. Olsson, K. Holmberg, B. Åkerman, Enzymes immobilized in mesoporous silica: A physical–chemical perspective, *Adv. Colloid Interface Sci.* 205 (2014) 339–360, <http://dx.doi.org/10.1016/j.cis.2013.08.010>.
- [47] S. Hudson, J. Cooney, E. Magner, Proteins in mesoporous silicates, *Angew. Chem. Int. Ed. Engl.* 47 (2008) 8582–8594, <http://dx.doi.org/10.1002/anie.200705238>.
- [48] F. Secundo, Conformational changes of enzymes upon immobilisation, *Chem. Soc. Rev.* 42 (2013) 6250–6261, <http://dx.doi.org/10.1039/c3cs35495d>.